Progressive Medial Axis Filtration

Noura Faraj   Jean-Marc Thiery   Tamy Boubekeur

Telecom ParisTech - CNRS LTCI - Institut Mines-Telecom
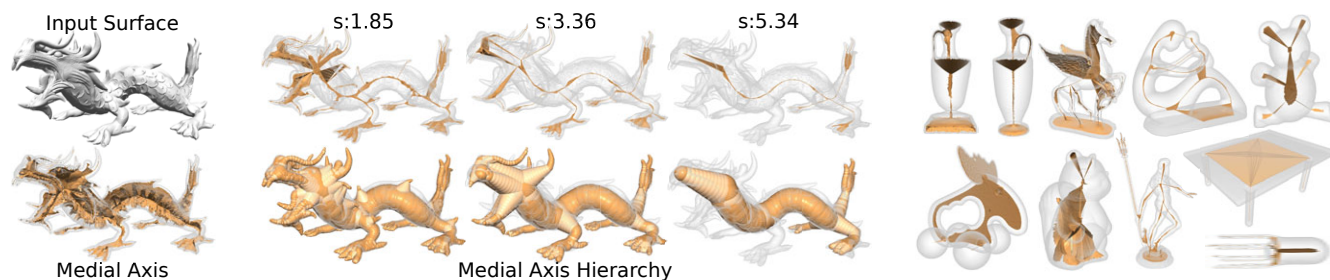
Figure 1: *Left – Dragon Model: Our progressive simplification of the medial axis filters the input shape at low scales (scale* 1.85*), and provides an efficient ordering of its features at large scales (scales* 3.36 *and* 5.34*). Top row shows the filtered medial axis, bottom row shows the polar (resp. interpolated) spheres in dark (resp. light) orange.* **Right:** *additional filtered medial axes.*

Abstract

The Scale Axis Transform provides a parametric simplification of the Medial Axis of a 3D shape which can be seen as a hierarchical description. However, this powerful shape analysis method has a significant computational cost, requiring several minutes for a single scale on a mesh of few thousands vertices. Moreover, the scale axis can be artificially complexified at large scales, introducing new topological structures in the simplified model. In this paper, we propose a progressive medial axis simplification method inspired from surface optimization techniques which retains the geometric intuition of the scale axis transform. We compute a hierarchy of simplified medial axes by means of successive edge-collapses of the input medial axis. These operations prevent the creation of artificial tunnels that can occur in the original scale axis transform. As a result, our progressive simplification approach allows to compute the complete hierarchy of scales in a few seconds on typical input medial axes. We show how this variation of the scale axis transform impacts the resulting medial structure.

CR Categories: I.3.5 [Computer Graphics]: Computational Geometry and Object Modeling—Hierarchy and geometric transformations;

Keywords: medial axis, scale axis, shape filtering

1 Introduction

In computer graphics applications, a 3D shape is typically modelled by its boundary, for which a number of representations exist and can be classified in either explicit (e. g., meshes, splines, points) or implicit (e. g., level sets, radial basis function) schemes. Medial structures such as the Medial Axis Transform [Blum 1967] (MAT) are located at the frontier between these two main classes of representations: the shape boundary is described by an inner structure together with a function conveying locally the volume of the shape. Such medial representations are particularly useful for shape analysis, see the work of Siddiqi et al. [Siddiqi and Pizer 2008] for more details.

The MAT $\mathcal{M}_{\mathcal{S}}$ of a 3D surface $\mathcal{S}$ is probably the most popular medial structure. This transform computes the set of "medial" spheres, contained in $\mathcal{S}$, with at least two contact points with $\mathcal{S}$. The spheres' center form the *medial axis*, which is made of 2-dimensional sheets, curves and single points, while a radius function describes, at each point, the maximally inscribed sphere. In this paper, we focus on polygonal surface meshes for which each connected component of $\mathcal{M}_{\mathcal{S}}$ is composed of triangles and/or edges.

The lack of stability of the MAT (i. e., small changes in the surface usually result in drastic changes in the medial axis), prevents from using it *directly* in applications (e. g., shape matching) and a specific filtering step is usually necessary. One popular method for this filtering operation is to simply remove spheres based on the angle formed by their two closest boundary points w.r.t. their center [Attali and Montanvert 1996]. Alternatively, some methods rely on the circumradius of the two closest boundary points to define the importance of a sphere [Chazal and Lieutier 2005].

The Scale Axis Transform [Giesen et al. 2009] [Miklos et al. 2010] (SAT) is a third approach targeting the filtering of the medial axis and relies on a spatially-varying *importance* measure of the features of the input shape. The SAT can be summarized as follow: **(i)** computation of the medial axis $\mathcal{M}_{\mathcal{S}}$ of the input surface $\mathcal{S}$; **(ii)** scaling of the medial spheres of $\mathcal{M}_{\mathcal{S}}$ by a factor s (the main input parameter); **(iii)** extraction of the corresponding surface $\mathcal{S}'$; **(iv)** computation of the medial axis $\mathcal{M}_{\mathcal{S}'}$ of $\mathcal{S}'$; **(v)** scaling of the medial spheres of $\mathcal{M}_{\mathcal{S}'}$ by a factor $1/s$. Intuitively, a sphere of $\mathcal{M}_{\mathcal{S}}$ is likely to be filtered during the scaling step if a significantly bigger sphere is close-by. The importance of a feature is then defined relatively to the size of the nearby geometry. In practice, the SAT generates simplified medial axes, with coarseness controlled by the scale parameter s. The topological events that can occur during the scaling step of the SAT are of two kinds: either a scaled sphere S_1 with radius sr_1 absorbs a smaller scaled sphere S_2 of radius sr_2 (*Simplification*, see Fig. 3 left), or two distincts spheres S_1 and S_2
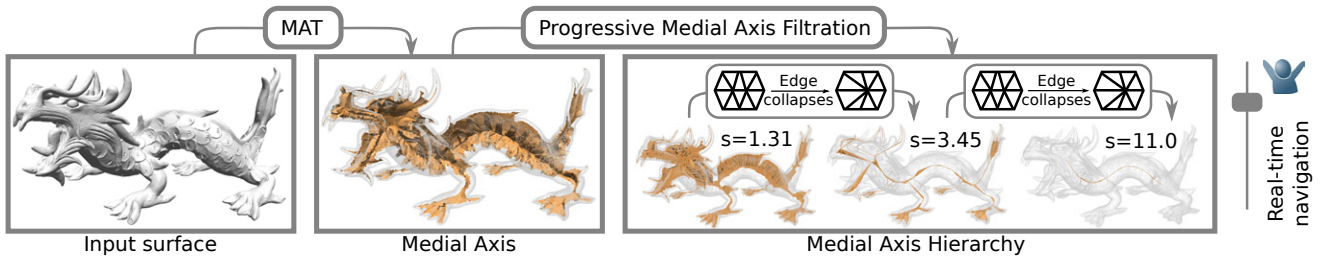
Figure 2: *Overview: Starting from a closed input surface (left), its medial axis is extracted (middle left) and simplified progressively by collapsing its edges iteratively (middle to right), constructing a medial axis hierarchy in a bottom-up fashion which can be quickly browsed.*
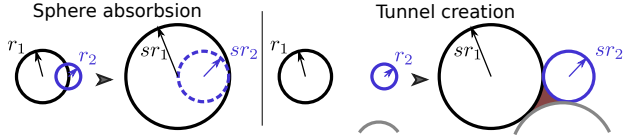

Figure 3: *Left: Simplification. Scaling the spheres by a factor s results in the absorbsion of S_2. Right: Enrichment. The scaling results here in the creation of a tunnel between S_1 and S_2.*

create a tunnel in the reconstructed surface when they touch each other (*Enrichment*, see Fig. 3 right). Formally, the various topological events occuring during the computation of the scale axis cannot be computed pair-wise only. Their exact computation involves all spheres to detect precisely if a grown sphere is covered (even partially) by the others, or if the point tangent to the two spheres at the creation of the tunnel is covered by another sphere (in which case no tunnel is created).

The main limitation of the SAT is threefold: first, computing a single scale requires the construction of an entire surface and the extraction of a specific medial axis, which prevents navigating easily the derived hierarchy in a reasonable amount of time; second, tunnels are likely to appear when the scale factor is too large, thus complexifying the topology of the medial axis instead of simplifying it; third, SAT spheres are not a subset of the medial axis ones.

We address these three problems by proposing an efficient medial axis simplification process which is based on the SAT importance metric, but which decimates the medial axis iteratively using an *edge-collapse* operator inspired from surface optimization [Garland and Heckbert 1997], without requiring any intermediate surface reconstruction/MAT during the process. As a result, a full hierarchy of nested medial structures can be generated in few seconds on typical inputs, and browsed interactively. As the edge-collapse is a decimation operator, no tunnels are created and each level can be expressed relatively to the next finer one and vise-versa (see Fig. 1).

2 Progressive Medial Axis Filtration

We summarize our approach in Fig. 2: starting from a closed surface $\mathcal{S}$, we extract its medial axis $\mathcal{M_S}$ using the same strategy as Miklos et al. [2010] and then simplify it progressively using of successive edge-collapses. The medial axis is stored in the data structure proposed by De Floriani et al. [2004], that allows to collapse edges of a non-manifold mesh efficiently. The resulting nested hierarchy guarantees that each of its levels is a simplification of the previous one and can be browsed interactively by the user.

The metric that guides the filtration focuses on the *Simplification* events introduced in Sec. 1 and omits the *Enrichment* events.

In the following, $\mathbf{v}_i$ denotes a vertex of $\mathcal{M_S}$, and represents a medial polar sphere with center $\mathbf{p}_i$ and radius r_i; $\mathbf{e}_{ij}$ denotes an edge of $\mathcal{M_S}$ linking $\mathbf{v}_i$ and $\mathbf{v}_j$. Our medial axis filtration algorithm is listed in Alg. 1, and has practical runtime and memory complexities of $\mathcal{O}(|\mathcal{M_S}|\log(|\mathcal{M_S}|))$.

Algorithm 1 Progressive Medial Axis Filtration.

Require: $\mathcal{M_S} = \{\{\mathbf{v}_i\}, \{\mathbf{e}_{ij}\}\}$ the medial axis of $\mathcal{S}$
Require: $\mathcal{Q}$ a priority queue of edges
Require: $\mathcal{R}$ an empty ordered list of edge-collapses
    for all edge $\mathbf{e}_{ij}$ **do**
        $\mathcal{Q} \leftarrow \mathbf{e}_{ij}$ with cost c_{ij}
    end for
    while $\mathcal{Q}$ **not** empty **do**
        $\mathbf{e}_{ij} \leftarrow \mathcal{Q}.top()$ with $r_i < r_j$; $\mathcal{Q}.pop()$
        if $\mathbf{v}_i$ valid **and** $\mathbf{v}_j$ valid **then**
            collapse $\mathbf{e}_{ij} \rightarrow \mathbf{v}_j$
            $\mathcal{R} \leftarrow [\mathcal{R}, [\mathbf{e}_{ij} \rightarrow \mathbf{v}_j]]$
            mark $\mathbf{v}_i$ as invalid
            for all neighbor $\mathbf{v}_k$ of $\mathbf{v}_j$ **do**
                $\mathcal{Q} \leftarrow \mathbf{e}_{jk}$ with cost c_{kj}
            end for
        end if
    end while
    return $\mathcal{R}$

One core idea of this paper is to define the cost that orders the edge collapses by the scale at which the largest sphere absorbs the other one:

$$c_{ij} = \frac{|\mathbf{p}_i \quad \mathbf{p}_j|}{|r_i \quad r_j|}$$

After inserting all possible edge collapse in $\mathcal{Q}$, we prune the element with the smallest cost iteratively and collapse the corresponding edge towards the largest sphere. Each time an edge is collapsed, the neighborhood of the created vertex is updated, and corresponding edge-collapses are inserted into the queue. Edges that were incident to the deleted vertex are invalidated in $\mathcal{Q}$ by invalidating the collapsed vertex. We stop when no edge remains in $\mathcal{M_S}$.

Similar to progressive meshes [Hoppe 1996], we record the set of deleted triangles and edges at each step of the simplification, constructing the nested hierarchy as an ordered list $\mathcal{R}$ where a medial axis at level k can be updated to level $k + 1$ (resp. k 1) using the kth (resp. k 1th) element of $\mathcal{R}$. As a result, the hierarchy can be traversed in real time, in both directions, using $\mathcal{R}$ only to obtain a specific scale s.
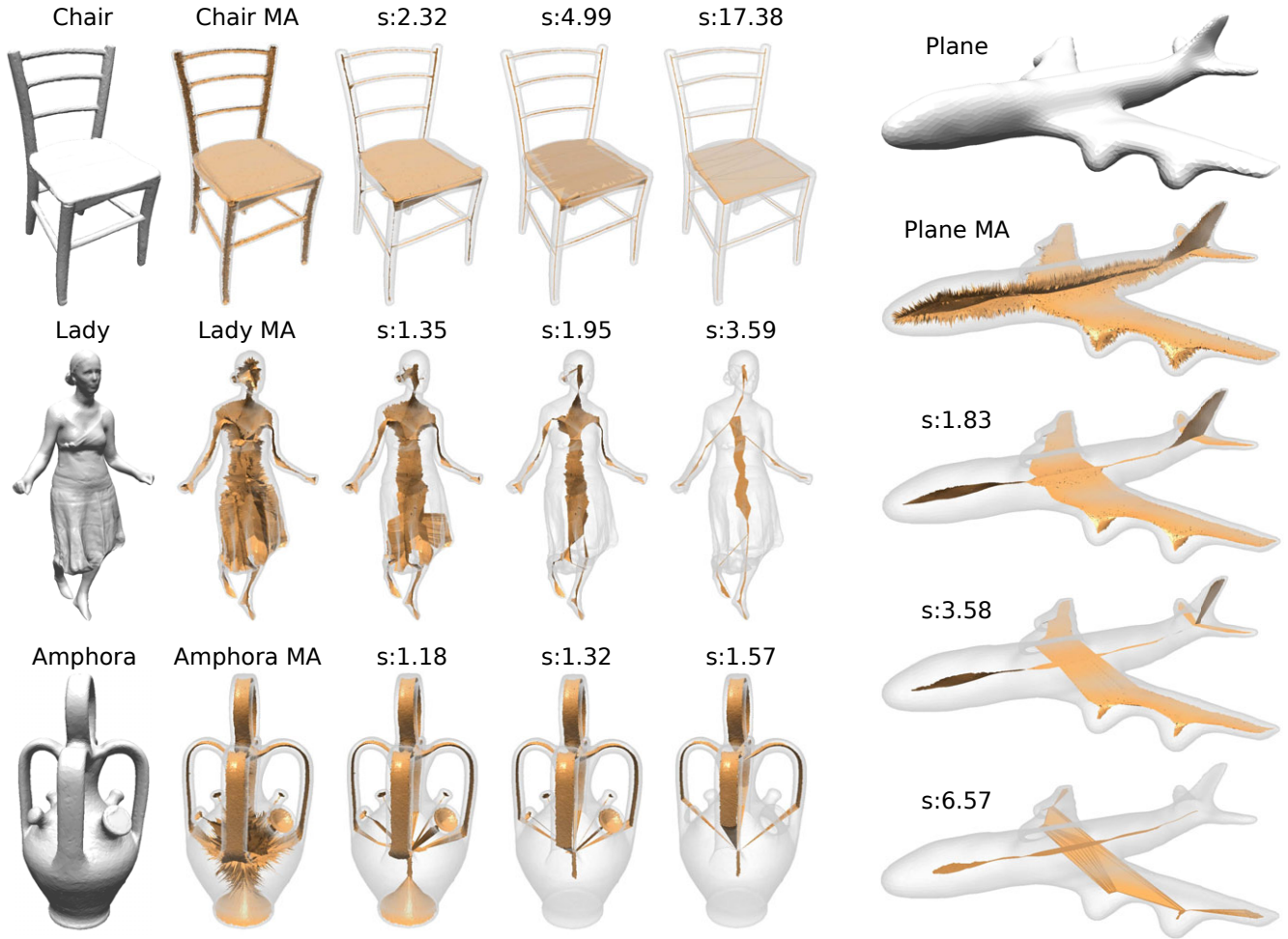
Figure 4: *Medial axis hierarchy extracted from various 3D shapes, with the input in grey, the medial axis (MA) and three different scales (s) obtained with our progressive simplication method. For illustration purpose, some medial axes are shown in wireframe.*

INPUT SURFACE (#V / #T)		MEDIAL AXIS (#V / #T / #E)	SECS.	OURS – ALL SCALES (SECS.)	SCALE	OURS H	SAT H	(SECS.)
Chair	(9935 / 19894)	(1014760 / 2289594 / 0)	627.90	68.23	2.32	1.02	1.20	(51.22)
					4.99	1.61	3.30	(13.1)
					17.38	2.50	12.77	(0.33)
Lady	(19990 / 39976)	(243400 / 532503 / 0)	75.70	15.20	1.35	1.65	2.11	(16.18)
					1.95	5.18	5.17	(5.39)
					3.59	7.95	7.66	(0.43)
Amphora	(14859 / 29734)	(141918 / 309993 / 0)	42.87	11.15	1.18	1.39	3.15	(13.84)
					1.32	3.72	4.52	(9.18)
					1.57	6.05	6.77	(5.43)
Plane	(6797 / 13590)	(253578 / 562181 / 0)	71.78	15.10	1.83	0.52	1.32	(17.38)
					3.58	2.46	3.59	(3.27)
					6.57	9.54	9.90	(0.77)

Table 1: *Timings for the computation of the complete simplification hierarchy, and Hausdorff distances (H) between surfaces reconstructed from various scales to the input surface. Timings for the computation of the Scale Axis Transform and Hausdorff distance to the input surface are given for each scale. Distances are expressed in percentages of the object's bounding box diagonal. All timings are expressed in seconds. The corresponding models are shown in Fig. 4.*

Figure 5: *Side by side visual comparison with the Scale Axis Transform (in purple).*

3 Results

Fig. 4 shows various medial axes simplified at several scales. Timings of computation of the whole hierarchy are reported in Tab. 1, along with the timings of computation of the Scale Axis Transform for the visualized scales. We also provide Hausdorff distances to the input surface for both methods. Since our technique is meant to filter large parts of the medial axis at large scales, these are given not to assess the quality of the simplification but rather to describe the size of the features that were removed.

The ability to navigate through the complete hierarchy in real-time allows the user to identify the key scales at which large features are filtered. Those values are impossible to predict beforehand, as illustrated by their variability in the presented examples.

As shown in Tab. 1, the computation of our all-scales simplification nested hierarchy is of the same order than the computation of a SAT for a single scale. Traversing the hierarchy and updating the medial axis simplification level is done in real-time on an Intel Core2 Duo running at 2.5 GHz with 4GB of main memory: going from 1 to 100.000 spheres takes a few milliseconds.

In Fig. 5 we illustrate the main differences with the SAT. Our progressive medial axis filtration behaves similarly to the SAT at low scales, but allows to filter features of the input medial axis at very large scales (10-30), for which the SAT does not provide useful information on the input shape [Miklos et al. 2010]. Even at medium scales, the SAT complexifies the shape instead of simplifying it (e. g., unwanted tunnels in the Hand model in Fig. 5–2nd row).

The spheres contained in our simplified medial axes are a subset of the polar spheres of the input medial axis. The primitives linking them (triangles, edges) are however not part of the input medial axis. Similarly to the SAT, our simplified medial axes can cross the input surface at very large scales. Nonetheless, this behavior is reduced with the proposed approach (see legs of the Raptor model in Fig. 5 – scales 5.62 and 7.85). Last, on the contrary to the SAT, our approach is free of computational parameters.

4 Conclusion

We have presented a technique for computing a progressive filtration of the medial axis, building upon the spatially-varying importance classification of the medial axis features introduced by the Scale Axis Transform [Miklos et al. 2010]. Our simplification process requires the computation of a single medial axis only, and progressively simplifies it using iterative edge-collapses, ordered by this importance classification, until no edge remains. The output of our technique is a nested hierarchy of medial structures that can be browsed interactively. Compared to the scale axis transform, a large number of level-of-detail medial structures can be quickly extracted, while we ensure the simplification of the medial axis at each step. Last, the information carried out by large simplification scales is pertinent and the algorithm is free of computational parameter.

References

ATTALI, D., AND MONTANVERT, A. 1996. Modeling noise for a better simplification of skeletons. In *Image Processing, 1996. Proceedings., International Conference on*, vol. 3, IEEE, 13–16.

BLUM, H. 1967. A Transformation for Extracting New Descriptors of Shape. In *Models for the Perception of Speech and Visual Form*, W. Wathen-Dunn, Ed. MIT Press, Cambridge, 362–380.

CHAZAL, F., AND LIEUTIER, A. 2005. The λ-medial axis. *Graphical Models 67*, 4, 304–331.

DE FLORIANI, L., MAGILLO, P., PUPPO, E., AND SOBRERO, D. 2004. A multi-resolution topological representation for non-manifold meshes. *Computer-Aided Design 36*, 2, 141–159.

GARLAND, M., AND HECKBERT, P. 1997. Surface simplification using quadric error metrics. In *Proceedings of the 24th annual conference on Computer graphics and interactive techniques*, ACM Press/Addison-Wesley Publishing Co., 209–216.

GIESEN, J., MIKLOS, B., PAULY, M., AND WORMSER, C. 2009. The scale axis transform. In *Proceedings of the Symposium on Computational geometry*, 106–115.

HOPPE, H. 1996. Progressive meshes. In *Proceedings of the 23rd annual conference on Computer graphics and interactive techniques*, ACM, 99–108.

MIKLOS, B., GIESEN, J., AND PAULY, M. 2010. Discrete scale axis representations for 3d geometry. *ACM Transactions on Graphics (TOG) 29*, 4, 101.

SIDDIQI, K., AND PIZER, S. M. 2008. *Medial representations: mathematics, algorithms and applications*, vol. 37. Springer.